MYC levels govern hematopoietic tumor type and latency in transgenic mice

Darrin P. Smith, Mary L. Bath, Donald Metcalf, Alan W. Harris, and Suzanne Cory

Deregulated MYC expression has been implicated in the etiology of many human cancers, including hematopoietic malignancies. To explore the impact of widespread constitutive MYC expression in the hematopoietic compartment, we have used a vector containing regulatory elements of the *Vav* gene to generate transgenic mice. VavP-*MYC* mice are highly tumor-prone and the level of MYC was found to influence both the kinetics and nature of the malignancies that developed. Whereas aggressive T-cell lymphomas rapidly overwhelmed the highest-expressing line, late-onset monocytic tumors greatly predominated in 2 low-expressing lines. These monocytic tumors most likely arise from abnormal macrophage colony-stimulating factor (M-CSF)–dependent progenitor cells having enhanced self-generative capacity. There appears to be a sharp threshold for MYC-induced T-cell lymphomagenesis because merely doubling the MYC level in a low-expressing line by breeding homozygous transgenic animals switched the phenotype from primarily monocytic tumors to exclusively T-cell tumors. Even the low level of *MYC*, however, clearly affected T-cell cycling, size, and sensitivity to apoptosis, and coexpression of a *BCL2* transgene promoted efficient T-cell lymphomagenesis. The implication is that MYC level affects the spontaneous acquisition of synergistic oncogenic mutations. (Blood. 2006;108:653-661)

Introduction

MYC is a transcription factor that activates or represses a wide spectrum of target genes.[1,2] In response to growth factors or cytokines, MYC levels are upregulated in the G_1 phase of the cell cycle to promote cell growth and transition into S phase.[3] Deregulated expression of MYC can also inhibit differentiation, induce genomic instability, and sensitize cells to apoptosis.[4,5] The apoptotic response is proposed to be a safety mechanism that deletes cells with deregulated, potentially oncogenic MYC.[6]

The role of MYC in human cancer was first established in Burkitt lymphoma, where chromosome translocation links *MYC* to immunoglobulin (Ig) loci and subjugates its expression to Ig enhancers.[7] MYC has now been implicated in the etiology of a wide variety of hematologic[8,9] and other malignancies.[3,10] The deregulating mutations impact either on *MYC* itself, as for example in translocations or amplifications, or on upstream regulatory pathways. The stability of MYC protein is tightly regulated, and the level of MYC may also be important during tumorigenesis, because secondary mutations that increase MYC stability have been observed for the translocated *MYC* allele in Burkitt lymphoma.[11-13]

Valuable insights into the mechanism of MYC-induced tumorigenesis have come from studies of transgenic mice, particularly the Eμ-*Myc* mouse,[14,15] which models the major chromosome translocation found in Burkitt lymphoma. In these mice, Myc is expressed under the control of the *IgH* enhancer (Eμ), and every mouse succumbs to a clonal pre-B or B-cell lymphoma, preceded by a benign proliferative phase during which expansion of the B lymphoid compartment is held within tolerable limits by apoptosis.[16,17] Lymphomagenesis in Eμ-*Myc* mice is markedly accelerated by the introduction of antiapoptotic mutations, as first demonstrated by overexpression of the prosurvival gene *BCL2*.[18] Furthermore, tumors arising spontaneously in Eμ-*Myc* mice carry mutations in the p19Arf-Mdm2-p53 pathway that disable p53-induced apoptosis.[19,20] The demonstration in transgenic mice that suppression of MYC can cause tumor regression[21] is encouraging the development of therapeutic strategies that target MYC or its upstream regulators.[22]

In order to assess the oncogenic impact of MYC in a wider range of hematopoietic cell types, we have generated several lines of transgenic mice in which *MYC* is expressed in a vector containing regulatory elements of the mouse *Vav* gene (VavP). The VavP transgene directs expression in every nucleated hematopoietic cell examined, including both differentiated and progenitor cells.[17,23,24] We have recently described the line with the highest expression (VavP-*MYC*17) in which the mice develop early-onset T lymphomas.[25] Here we characterize 3 further lines of VavP-*MYC* mice, and show that MYC provokes very different tumor phenotypes depending on the level of its expression. Furthermore, we show that MYC has marked effects on the development of megakaryocytes and macrophages.

From The Walter and Eliza Hall Institute of Medical Research, Melbourne, Victoria, Australia.

Submitted January 17, 2006; accepted February 28, 2006. Prepublished online as *Blood* First Edition Paper, March 14, 2006; DOI 10.1182/blood-2006-01-0172.

Supported by the National Health and Medical Research Council (NHMRC; Canberra, program grant 257502), the National Cancer Institute (grant CA43540), and the Leukemia and Lymphoma Society (Specialized Center of Research grant 7015).

D.P.S. and D.M. designed and performed research, analyzed data and wrote the paper; M.L.B. designed and performed research and analyzed data; A.W.H. designed research and analyzed data; and S.C. designed research, analyzed data, and wrote the paper.

An Inside *Blood* analysis of this article appears at the front of this issue.

Reprints: Suzanne Cory, The Walter and Eliza Hall Institute of Medical Research, 1G Royal Parade, Melbourne, Victoria 3050, Australia; e-mail: cory@wehi.edu.au.

The publication costs of this article were defrayed in part by page charge payment. Therefore, and solely to indicate this fact, this article is hereby marked "advertisement" in accordance with 18 U.S.C. section 1734.

Materials and methods

VavP-*MYC* mice

All experiments were carried out in accordance with the National Health and Medical Research Council (Canberra, Australia) Code of Practice for the Care and Use of Animals for Scientific Purposes (2004) and approved by the Melbourne Health Research Directorate Animal Ethics Committee.

All mice were of the C57BL/6J (B6) background and bred in the facilities of this institute. Transgene construction and the generation of VavP-*MYC* mice by pronuclear injection were as previously described.[25] Three lines were bred from primary VavP-*MYC* mice: *MYC*17 (with 11 copies of the transgene), *MYC*10 (7 copies), and *MYC*12 (3 copies). Transgenic offspring were identified by polymerase chain reaction (PCR) of DNA prepared from tail biopsies or blood using primers to the vector SV40 polyadenylation signal (forward: gccgcagacatgataagatacatt; reverse: tcggctcgcgaggttttac).

Mice homozygous for the VavP-*MYC*10 locus (*MYC*10^{hom} mice) were generated by crossing *MYC*10 mice. Quantitative slot-blotting of tail biopsy DNA was used to distinguish wild-type, *MYC*10, and *MYC*10^{hom} littermates. Tail DNA was quantified using a fluorometer after staining with Hoechst 33258 and then 6 μg of denatured DNA was slot-blotted onto nylon membranes and fixed by ultraviolet (UV) irradiation. The ^{32}P-labeled probe was prepared by random primer labeling of a 323-bp fragment of the VavP-*MYC* transgene (generated by PCR with the primers gcggccgcagacatgataa and actagtggatccgctggcg). The membrane was prehybridized and hybridized at 65°C in modified Church and Gilbert buffer (7% SDS, 10 mM EDTA, 0.5 M sodium phosphate [pH 7.2], and 100 μg/mL sonicated and denatured salmon sperm DNA) and washed at 65°C in 0.5 × standard saline citrate (SSC; 1× = 150 mM sodium chloride and 15 m sodium citrate, pH 7.0)/0.1% SDS.

Bitransgenic *MYC*10-*BCL2*.69 mice were generated by in vitro fertilization[26] of eggs from approximately 4-week-old VavP-*MYC*10 mice using sperm from VavP-*BCL2*.69 mice. The VavP-*MYC* transgene was detected by PCR using a forward primer to the *MYC* cDNA (ccaagcagaggagcaaagctcatt) and the reverse SV40 polyadenylation signal primer. VavP-*BCL2*.69 mice were identified by their high blood-leukocyte count[27] determined with a Coulter Z2 particle count and size analyzer (Beckman-Coulter, Miami, FL).

Platelet numbers and size were determined with a hematology analyzer (Advia 120; Bayer, Tarrytown, NY). Tumor transplantation tests and histologic analyses were performed as previously described.[25] Sections were stained with hematoxylin and eosin (H&E), mounted in Safety Mount No. 4 (Fronine, Sydney, Australia), and observed using an Optiphot microscope (Nikon, Tokyo, Japan) with Plan Apo × 40 (NA 0.95) or Plan Apo × 100 (NA 1.35, oil) objective lenses. Images were captured with a Nikon DS camera head (DS-5M; Nikon, Melville, NY) and control unit (DS-L1) using integral software.

Expression analysis

Western blots were performed using 40 μg of protein extract per lane as previously described[25] but using a different rabbit MYC antibody (no. 11917; Abcam, Cambridge, United Kingdom). For reverse transcriptase (RT)–PCR, total cellular RNA was prepared from cell suspensions using the QIAshredder, RNeasy mini kit, and RNase-Free DNase set (Qiagen, Hilden, Germany) as described by the manufacturer. For each RNA sample, 4 25-μL OneStep RT-PCR reactions (Qiagen) were carried out using serially 5-fold less RNA (100 ng, 20 ng, 4 ng, and 0.8 ng). Reverse transcription was at 50°C for 30 minutes, followed by heat inactivation at 95°C for 15 minutes. PCR products were synthesized using 35 cycles of 94°C for 30 seconds, 64°C for 30 seconds, 72°C for 60 seconds, and resolved on 2% agarose gels. Transgene-expressed human *MYC* RNA was detected as a 379-bp PCR product synthesized using a forward primer (accagaaagttaactggcctgtacg) spanning VavP vector exonic sequences either side of the SV40 late intron and a reverse primer (accatctccagctggtcgg) in *MYC* cDNA. Endogenous β-*Actin* RNA was detected as a 688-bp product synthesized using a forward primer in exon 1 (ctttgcagctccttcgttgc) and a reverse primer in exon 4 (ctctttgatgtcacgcacgatttc).

Flow cytometry and cell-cycle analysis

Flow cytometry and sorting was performed as previously described.[25] For cell-cycle analyses, 2.5×10^5 sorted thymocytes were stained with propidium iodide (100 μg/mL) in 400 μL of hypotonic buffer (10 mM Tris-HCl [pH 8], 1 mM NaCl, 0.1% [vol/vol] NP-40, and 10 μg/mL RNase A) at 4°C for 60 minutes. Flow cytometric data were analyzed with the ModFit LT 3.0 program (Verity Software House, Topsham, ME) to determine the proportions of cells in the G_0/G_1, S, and G_2/M phases of the cell cycle.

Thymocyte survival assays

Thymocytes (1×10^6) were cultured in 24-well plates in 1 mL Dulbecco modified Eagle medium (DMEM) supplemented with 10% fetal calf serum (FCS), 100 μM L-asparagine and 50 μM 2-mercaptoethanol. Following 0, 1, 2, and 3 days in culture, replicate wells were harvested and the cells transferred to tubes containing 20×10^3 10-μm-diameter latex beads (Beckman-Coulter) and surface-stained with biotin–anti-CD4/streptavidin-PE and FITC–anti-CD8. The cell and latex-bead mixture was washed and resuspended in 200 μL balanced salt solution containing 2% FCS and 2 μg/mL propidium iodide. For flow cytometry, the latex beads were detected in a forward–versus–side light scatter gate and data were acquired until 4×10^3 beads had been counted. The number of viable (unstained by propidium iodide) $CD4^+$ $CD8^+$, $CD4^+$ $CD8^-$, and $CD4^-$ $CD8^+$ thymocytes acquired per sample was determined, and the proportion relative to day 0 in culture calculated.

Colony-forming assays

Marrow cells (2.5×10^4) were cultured for 7 days in 1 mL DMEM containing 20% newborn calf serum and 0.3% agar and cytokines, as previously described.[28] Cytokines were purified recombinant murine molecules (PeproTech, Rocky Hill, NJ) or recombinant human granulocyte (G)–CSF (Amgen, Thousand Oaks, CA), used at the following concentrations: G-CSF, M-CSF, granulocyte-macrophage (GM)–CSF, interleukin-3 (IL-3), and leukemia inhibitory factor (LIF) at 10 ng/mL; stem-cell factor (SCF) and IL-6 at 100 ng/mL; erythropoietin (EPO) at 2 IU/mL; thrombopoietin (TPO) at 50 ng/mL; interferon γ (IFNγ) at 2000 U/mL; and FMS-like tyrosine kinase 3 ligand (Flt3L) at 500 ng/mL. Differential colony counts were performed on fixed whole-mount preparations stained for acetylcholinesterase and with Luxol fast blue and hematoxylin. For recloning studies, individual 7-day colonies were resuspended in 8 mL of agar medium and then cultured for 7 days in duplicate dishes.

Results

VavP-*MYC* mouse lines differ in transgene expression levels

Three lines of mice were generated by pronuclear microinjection of human *MYC* cDNA in a *Vav* enhancer/promoter vector (VavP-*MYC*17, VavP-*MYC*10, and VavP-*MYC*12 mice; hereafter referred to as *MYC*17, *MYC*10, and *MYC*12 mice), and a fourth line was produced by breeding mice homozygous for the *MYC*10 locus (*MYC*10^{hom} mice). Analysis of MYC protein levels in thymocytes from young healthy mice (Figure 1A) indicated that the expression level varied significantly between these lines (*MYC*17 > *MYC*10^{hom} > *MYC*10 > *MYC*12). As reported for Eμ-*Myc* transgenic mice,[29] expression of endogenous MYC was effectively repressed, even in the line with the lowest expression (Figure 1A), presumably due to a negative feedback mechanism.

*MYC*17 mice have been shown previously by Western blotting to express the transgene in the B, T, and myeloid lineages, with expression being highest in the T lineage.[25] In the lower-expressing transgenic lines protein expression was not readily detected outside the T lineage, but RT-PCR analysis of tissues and cells from

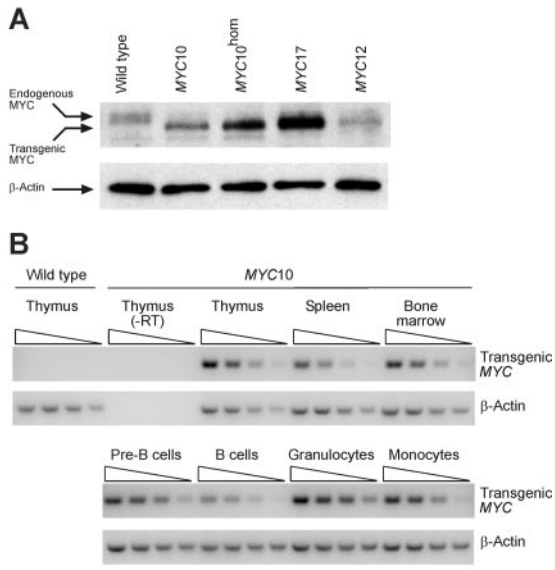

Figure 1. VavP-*MYC* lines with a range of transgene expression levels. (A) Differing expression levels of transgenic MYC protein in *MYC*17, *MYC*10, *MYC*10^{hom} (homozygous for the transgene locus), and *MYC*12 mice. Western blot of thymocyte lysates prepared from healthy young transgenic and wild-type mice were probed with anti-MYC antibody. Note that expression of endogenous Myc (a slower-migrating, broad, phosphorylated band) is repressed in the transgenic samples. The same filter probed with anti–β-actin is shown as a loading control. (B) Widespread expression of transgenic *MYC* RNA in *MYC*10 mice. Semiquantitative RT-PCR analysis of RNA prepared from thymocytes, splenocytes, bone marrow cells, and sorted pre-B cells (B220$^+$ IgM$^-$), B cells (B220$^+$ IgM$^+$), monocytes (Mac1$^+$ Gr1$^-$), and granulocytes (Mac1$^+$ Gr1$^+$) from 8-week-old *MYC*10 mice. Analyses of RNA with the reverse transcription reaction omitted (−RT) confirms specificity of PCR primers for transgene-expressed *MYC* RNA. RT-PCR reactions from serial 5-fold dilutions of input RNA are shown. Analysis of endogenous β-*Actin* RNA is shown as a control.

*MYC*10 mice (Figure 1B) indicated that the transgene was expressed in thymocytes, splenocytes, bone marrow cells, and in sorted populations of pre-B cells (B220$^+$ IgM$^-$), B cells (B220$^+$ IgM$^+$), monocytes (Mac1$^+$ Gr1$^-$), and granulocytes (Mac1$^+$ Gr1$^+$). RNA levels were somewhat lower in B cells (and, correspondingly, in the spleen) than in the other cell types.

Rate of tumorigenesis and tumor type correlates with transgene expression levels

All mice in each of the 4 lineages succumbed to tumors within the first 18 months of life and, significantly, median survival was inversely proportional to the level of MYC. The line with the lowest expression, *MYC*12, had a median survival of 58 weeks compared with 41 weeks for *MYC*10 mice, 13 weeks for *MYC*10^{hom} mice, and 8 weeks for *MYC*17 mice (Figure 2).

In marked contrast to the *MYC*17 mice, which succumbed to very early onset T-cell lymphoma,[25] all *MYC*12 mice autopsied (n = 24) and 93% of the *MYC*10 mice (n = 112) developed tumors with the histologic appearance of histiocytic sarcoma (Figure 3A).[30] All tumors analyzed by flow cytometry (10 from *MYC*10 mice and 5 from *MYC*12 mice) expressed the myeloid markers F4/80 and Mac1 but not the granulocyte marker Gr1 (Figure 3B). They were also negative for B-lineage markers, including B220 and CD19; T-lineage markers, including Thy1 and CD3; and the erythroid marker Ter119 (Figure 3B; not shown). The histiocytic sarcomas were therefore tumors in the monocyte or macrophage lineage.

In the *MYC*10 mice, the macrophage tumors were widely disseminated throughout the hematopoietic tissues, with large deposits in 1 or more lymph nodes and also in the spleen, bone marrow, and thymus (90%, 80%, 60%, and 40% of mice, respectively). Tumor infiltration of the liver, lung, and kidney was frequent (80%, 70%, and 40% of mice, respectively). In addition, 40% of the mice had deposits that had spread locally through the dermis, hypodermis, muscle, and fat of the skin. In the *MYC*12 mice, similar cutaneous histiocytic tumors were the primary feature (80% of cases) and deposits elsewhere (in hematopoietic tissues, liver, lung, and kidney) were variable and generally less extensive than in *MYC*10 mice. None of the histiocytic tumors was accompanied by monocytic leukemia, but granulocytosis (presumably as a response to tumor[15]) was sometimes noted. Of the 5 *MYC*10 tumors tested, all were transplantable.

A small proportion of *MYC*10 mice (7%) succumbed to lymphoblastic lymphoma rather than histiocytic sarcoma. Significantly, these tumors were earlier in onset and all 5 were T-cell lymphomas; they expressed the T-lineage markers Thy1, TCRβ, and CD3, and lacked CD19, Ter119, and Mac1 (not shown). Four were CD4$^+$ CD8$^+$ pre–T-cell lymphomas, and 1 was a CD4$^+$ CD8$^-$ mature T-cell lymphoma. These tumors resembled the T-cell lymphomas seen in the high expressing (*MYC*17) line,[25] which developed mostly CD4$^+$ CD8$^-$ and a significant minority of CD4$^+$ CD8$^+$ lymphomas.

The observations that most of the tumors arising in the 2 lowest-expressing lines were slow-developing macrophage tumors, and that the few early-onset tumors were T-cell lymphomas, as in the high-expressing (*MYC*17) line,[25] suggested that there might be a threshold level of MYC expression required for efficient T-cell lymphomagenesis. We tested this directly by ascertaining the tumor susceptibility of *MYC*10^{hom} mice, which expressed approximately twice as much MYC in thymocytes as *MYC*10 mice (see Figure 1A). Significantly, *MYC*10^{hom} mice had a greatly shortened lifespan compared with *MYC*10 mice (median of 13 weeks rather than 41 weeks) and all succumbed to T-cell lymphoma. The 21 tumors analyzed histologically were all lymphoblastic in morphology (Figure 3C), and by flow cytometric analysis 20 were CD4$^+$ CD8$^+$ pre–T-cell lymphomas (Figure 3D), and 1 was a CD4$^+$ CD8$^-$ mature T-cell lymphoma. The tumors presented as a grossly enlarged thymus (apart from the mature T-cell lymphoma) and the involvement of other organs was variable, except for the few leukemic mice (15%), which had extensive tumor infiltration of many organs. In occasional mice (15%), patches of histiocytic sarcoma were also apparent histologically.

Preneoplastic changes primarily affect megakaryocytes and macrophage precursors

In contrast to the marked preneoplastic phenotype of *MYC*17 mice,[25] that of *MYC*10 and *MYC*10^{hom} mice were relatively mild.

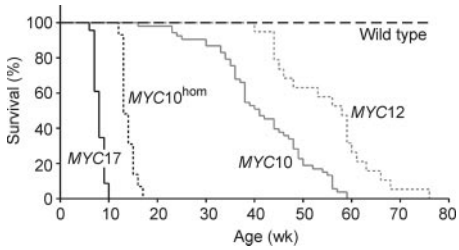

Figure 2. Tumorigenesis in VavP-MYC mice. *MYC*10 (n = 53), *MYC*10^{hom} (n = 29), *MYC*12 (n = 19), *MYC*17 (n = 23; data from Smith et al[25]), and wild-type (B6) (n = 25) mice were monitored for tumors and killed when sick. The percentage of mice surviving at weekly intervals is shown. Log-rank analysis comparing wild-type versus *MYC*12, *MYC*12 versus *MYC*10, *MYC*10 versus *MYC*10^{hom}, and *MYC*10^{hom} versus *MYC*17 showed that in all cases survival was significantly different ($P < .001$).

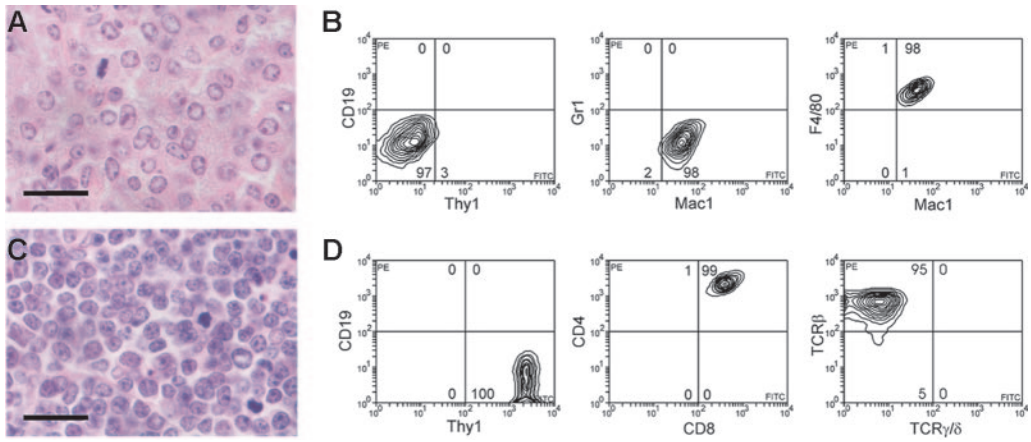

Figure 3. Distinct tumor types in *MYC*10 and MYC10^{hom}mice. (A) High-power view of a *MYC*10 thymic macrophage tumor, comprising large cells with bulky, variably vacuolated cytoplasm and a vesicular, sometimes pleomorphic nucleus, characteristics of histiocytic sarcoma. H&E-stained section; scale bar equals 20 μm. (B) Flow cytometric analysis of typical *MYC*10 macrophage (Mac1$^+$ F4/80$^+$ Gr1$^-$ CD19$^-$ Thy1$^-$) tumor. The percentage of cells in each quadrant is indicated. (C) High-power view of a thymic *MYC*10^{hom} pre–T-cell lymphoma with lymphoblastic morphology, comprising smaller cells with indistinct cell borders. (D) Flow cytometric analysis of typical *MYC*10^{hom} pre–T-cell (Thy1$^+$ TCRβ$^+$ CD4$^+$ CD8$^+$ CD19$^-$) lymphoma.

Flow cytometry indicated a generally modest increase in the frequency of all cell types analyzed in the spleen (pre-B cells, B cells, CD4$^+$ CD8$^-$ and CD4$^-$ CD8$^+$ T cells, monocytes, granulocytes, and erythroid cells), and the increase was greater for *MYC*10^{hom} than *MYC*10 mice (Table 1). Cell numbers were near normal in the bone marrow, thymus, and blood (not shown) but many cell types were slightly enlarged, including pre-B cells, B cells, CD4$^+$ CD8$^-$ and CD4$^-$ CD8$^+$ T cells, and monocytes (Figure 4B; not shown).

Megakaryocytopoiesis was strikingly abnormal in VavP-*MYC* mice. In *MYC*17 mice, there were substantially more megakaryocytes in the spleen at 2 weeks (Smith et al[25]; Table 2) and in the bone marrow by 4 weeks (Table 2). Megakaryocyte numbers were also significantly increased in the spleen and bone marrow of *MYC*10^{hom} mice, but not *MYC*10 mice (Table 2). Notably, the megakaryocytes were consistently larger (Table 2) and they had a more complex nucleus. Further histologic examination revealed that in *MYC*17, *MYC*10^{hom}, and to a lesser extent, *MYC*10 mice, many megakaryocytes in the bone marrow contained other leukocytes, almost all of them intact granulocytes (Figure 5A; Table 2), presumably as a result of emperipolesis ("Discussion"). Concomitant with megakaryocyte abnormalities, *MYC*10^{hom} and *MYC*17 mice produced a reduced number of circulating platelets (approximately 2-fold and 5-fold fewer, respectively) and those present were larger, but there was little change in *MYC*10 mice (Table 2).

To ascertain myeloid and megakaryocyte progenitor- and preprogenitor-cell numbers, bone marrow cells from *MYC*17 and *MYC*10 mice were cultured in semisolid medium in the presence of 12 different cytokines or combinations thereof. The frequency of different colony types that grow in such assays reflects the size and composition of the progenitor-cell compartment. In control cultures containing no added stimulus, no colonies developed, indicating that enforced expression of MYC had not conferred cytokine independence. In the presence of exogenous cytokines, colony number and composition were normal, with 1 remarkable exception: Cultures stimulated by M-CSF developed prominent, abnormally large, compact macrophage colonies (80% of colonies in *MYC*17 cultures and 50% of colonies in *MYC*10 cultures; Figure 5B). Furthermore, the total number of macrophage colonies was significantly increased in the bone marrow of *MYC*17 and, to a lesser degree, *MYC*10 mice (Table 3). The macrophage nature of these colonies was confirmed by flow cytometry; the cells were all strongly positive for the macrophage marker Mac1 but negative for T- and B-cell markers (CD3 and B220, respectively).

Titration experiments established that the quantitative responsiveness to M-CSF of MYC-expressing progenitor cells, including those capable of producing large colonies, was comparable to that of normal M-CSF–dependent progenitors (not shown). Recloning experiments were then undertaken to determine how many cells in

Table 1. Altered composition of the spleen in healthy young *MYC*10 and *MYC*10^{hom} mice

	Cell no. per spleen, × 10^{6}*				
Cell type	Wild-type	*MYC*10	Ratio† (*P*)	*MYC*10^{hom}	Ratio† (*P*)
Total	180 ± 20	240 ± 20	1.3 (.03)	310 ± 40	1.7 (.01)
Pre-B	2.9 ± 0.3	4.1 ± 0.5	1.4 (.06)	7.2 ± 0.1	2.5 (< .01)
B	110 ± 10	140 ± 10	1.3 (.03)	190 ± 20	1.7 (.01)
CD4$^+$ CD8$^-$ T	31 ± 4	42 ± 2	1.4 (.03)	44 ± 2	1.4 (.02)
CD4$^-$ CD8$^+$ T	18 ± 2	24 ± 2	1.3 (.06)	24 ± 2	1.3 (.07)
Erythroid	0.9 ± 0.3	2.8 ± 0.6	3.1 (.02)	9.5 ± 3.2	10.6 (.03)
Monocyte	5.2 ± 0.8	6.4 ± 0.4	1.2 (.13)	8.6 ± 1.1	1.7 (.03)
Granulocyte	4.0 ± 0.2	4.5 ± 0.6	1.1 (.23)	10 ± 3	2.5 (.04)

Eight-week-old mice were analyzed. Total nucleated counts were determined with a Coulter counter and subpopulations by flow cytometry. Cell types examined were pre-B (B220$^+$ IgM$^-$), B (B220$^+$ IgM$^+$), erythroid (Ter119$^+$), granulocyte (Gr1$^+$ Mac1$^+$), monocyte (Gr1$^-$ Mac1$^+$), and T-cell subpopulations (based on CD4/CD8 expression). *P* for a *t* test.

*Mean ± SEM; n = 3.

†Ratio of *MYC*10 or *MYC*10^{hom} to wild-type control.

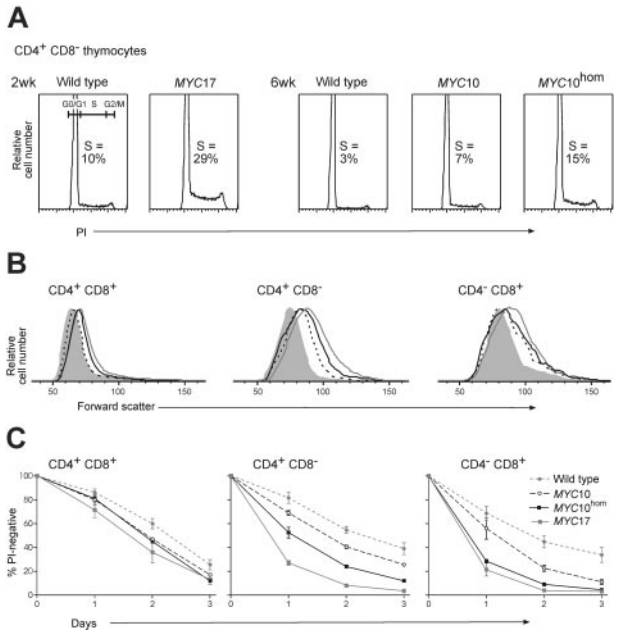

Figure 4. VavP-*MYC* transgene expression has multiple effects on thymocytes. (A) Proliferation is increased. Sorted thymocyte subpopulations from healthy young mice were permeabilized, stained for DNA content with propidium iodide (PI), and analyzed by flow cytometry. Representative cell-cycle profiles for $CD4^+$ $CD8^-$ T cells show an increased proportion of cells in S phase in VavP-*MYC* transgenic mice, and the cell-cycle distributions of all the thymocyte subpopulations analyzed is shown in Table 4. (B) Cell size is increased. Forward light-scatter analysis of gated thymocyte subpopulations from healthy young mice (2-week-old *MYC*17 and 6-week-old *MYC*10, *MYC*10^{hom}, and wild-type mice). Representative examples from 3 mice or more examined are shown; wild-type thymocyte size was comparable at 2 and 6 weeks. Gray filled indicates wild-type; black dashed line, *MYC*10; black solid line, *MYC*10^{hom}; and gray solid line, *MYC*17. (C) Sensitivity to spontaneous apoptosis is increased. Thymocytes from healthy young mice (2- and 6-week-old wild-type, 2-week-old *MYC*17, and 6-week-old *MYC*10 and *MYC*10^{hom} mice) were cultured in vitro in simple medium. The percentage of gated thymocyte subpopulations remaining viable (not stained with propidium iodide) after 1 to 3 days was determined by flow cytometry (assays were performed on 2 or more independent cultures from each of 2 or more mice of each genotype; mean percentages ± SEM are for replicate mice).

the abnormally large colonies retained clonogenic potential (Figure 5C). Colonies grown in M-CSF were resuspended and recultured with M-CSF in semisolid medium. As expected, primary colonies from wild-type mice contained very few clonogenic cells: on average, each produced only 300 small colonies or clusters, and when recloning was repeated sequentially for a second and third cycle almost no colonies developed. In marked contrast, giant colonies from *MYC*10 mice contained an average of 2000 cells able to form compact secondary colonies, although these were smaller than the primary colonies. In subsequent rounds of recloning, however, there was an abrupt fall to an average of 150 clonogenic cells per colony in the second cycle, and only 10 per colony in the third cycle. These data imply that the *MYC*10 progenitor cells forming giant colonies lacked capacity for full self-renewal, but did have a significantly extended capacity for self-generative divisions.

MYC expression increases thymocyte proliferation, size, and sensitivity to apoptosis

As efficient T-cell lymphomagenesis appeared to require a threshold level of transgenic MYC expression, we surveyed the impact of the various levels of MYC expression on thymocytes from healthy young mice.

Cells from *MYC*17 mice were analyzed at approximately 2 weeks, an age when they reliably lack tumor cells, as judged by flow cytometry, histology, or transplantation (not shown). As expected from the susceptibility of this line to early T lymphomas,[25] the T cells in young *MYC*17 mice displayed multiple changes. Cell-cycle analysis showed that more $CD4^+$ $CD8^+$ pre-T cells and especially $CD4^+$ $CD8^-$ thymocytes were in S phase than in control wild-type littermates (Figure 4A; Table 4). (The increased cycling was not as marked for $CD4^-$ $CD8^+$ thymocytes, probably because a striking 40% of these cells were already in S phase in 2-week-old control mice.) Another notable difference was that pre-T, $CD4^+$ $CD8^-$, and $CD4^-CD8^+$ thymocytes from *MYC*17 mice were substantially larger (Figure 4B; Smith et al[25]), and much more susceptible to spontaneous apoptosis when cultured without cytokine support (Figure 4C).

Thymocytes from *MYC*10 and *MYC*10^{hom} mice were similarly compared with those from wild-type littermate control mice at the oldest age (approximately 6 weeks) reliably lacking detectable tumor cells. The impact of the transgene was generally less than in *MYC*17 mice but nonetheless clear, even in *MYC*10 mice, which rarely develop T-cell tumors. The number of pre-T, $CD4^+$ $CD8^-$, and $CD4^-$ $CD8^+$ thymocytes in S phase increased, and the increase was more pronounced in *MYC*10^{hom} mice (Figure 4A; Table 4). The effect on $CD4^+$ $CD8^-$ cells was most notable, with *MYC*10 mice having approximately twice as many, and *MYC*10^{hom} mice approximately 5 times as many of these cells in S phase as controls. The size of thymocytes within all 3 subpopulations was also increased (Figure 4B), and again the impact was greater for *MYC*10^{hom} mice. Finally, the 3 thymocyte subpopulations analyzed were all more

Table 2. Megakaryocyte and platelet abnormalities in healthy young VavP-*MYC* mice

	Bone marrow megakaryocytes			Spleen megakaryocytes	Platelets§	
	No.*	Size, mm†	Internalized cells, %‡	No.*	× 10^7/mL	Vol, fL
Wild-type, 2-4 wk	4.7 ± 0.5	23 ± 2	2	3.6 ± 0.4	104 ± 13	5.3 ± 0.1
*MYC*17, 2-4 wk‖	7.2 ± 0.5	46 ± 2	57	7.1 ± 0.6	20 ± 3	8.4 ± 0.6
Wild-type, 5-7 wk	6.2 ± 0.6	29 ± 1	0	1.9 ± 0.3	130 ± 7	5.8 ± 0.1
MYC10^{het}, 5-7 wk	7.1 ± 0.4¶	38 ± 1‖	20‖	2.0 ± 0.3¶	113 ± 6¶	6.2 ± 0.1‖
MYC10^{hom}, 5-7wk‖	9.5 ± 0.6	50 ± 2	58	3.4 ± 0.4	49 ± 3	7.1 ± 0.1

*Mean frequency in tissue sections (± SEM) per high-power (× 400) microscope field. For each tissue, 20 to 48 fields were counted from 3 to 6 mice of each genotype and age. For *MYC*17 mice, the spleen was analyzed at 2 weeks and bone marrow was analyzed at 4 weeks. Note: the overall increase in splenic megakaryocytes in *MYC* mice is greater than suggested by these field counts because the average spleen size is larger than wild-type controls (3-fold for *MYC*17, approximately 1.3-fold for *MYC*10^{het}, and 1.7-fold for *MYC*10^{hom} mice). *P* for a *t* test.

†Mean megakaryocyte diameter in tissue sections (± SEM); n = 60.

‡The percentage of megakaryocytes (n = 60) in tissue sections containing internalized cells (mainly intact granulocytes). The mean number of internalized cells per megakaryocyte section containing such cells was 2.6 ± 0.4 for *MYC*17, 1.2 ± 0.1 for *MYC*10^{het}, and 2.1 ± 0.2 for *MYC*10^{hom}.

§Mean platelet counts (± SEM) and mean platelet volume (± SEM) in blood samples (n = 4-14).

‖$P \leq .001$.

¶$P \geq .05$.

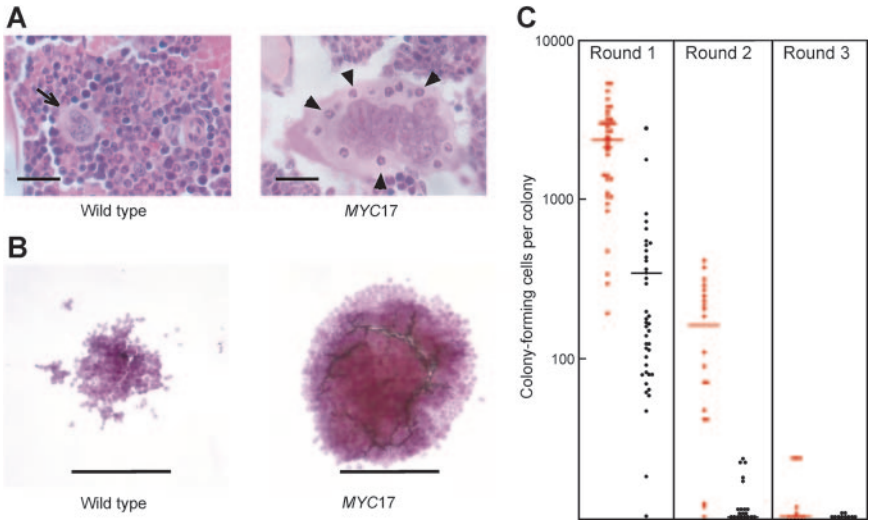

Figure 5. Abnormal hematopoiesis in VavP-*MYC* mice. (A) An abnormally large megakaryocyte in the bone marrow of a 4-week-old *MYC*17 mouse (right panel) containing internalized granulocytes (some indicated by arrowheads) and for comparison, a normal megakaryocyte (left panel; indicated by arrow) in the bone marrow of a wild-type littermate. H&E-stained sections; scale bar equals 20 μm. (B) Abnormally large macrophage colonies developed in M-CSF–stimulated cultures of *MYC*17 (right panel) and *MYC*10 (not shown) bone marrow cells when compared with cultures of wild-type cells (left panel); scale bar equals 125 μm. (C) Primary M-CSF–stimulated macrophage colonies from 8-week-old *MYC*17 (red) and wild-type (B6) mice were recultured in M-CSF (Round 1) and the colonies that developed were counted. Recloning was performed for 2 more successive rounds using colonies from the first and second rounds. Bars indicate the mean.

sensitive to spontaneous apoptosis (Figure 4C), pre-T thymocytes being the least and $CD4^-$ $CD8^+$ thymocytes the most sensitive, particularly for *MYC*10^{hom} cells.

Overall, these data indicate that constitutive expression of MYC in T cells increases cell cycling, size, and sensitivity to apoptosis even when expression is below a critical threshold required for efficient progression to malignancy, and that the impact of MYC is proportional to its level of expression.

Overexpression of BCL2 facilitates T-cell lymphomagenesis in *MYC*10 mice

BCL2 synergizes with Myc in transforming B-lymphoid cells.[18] We sought to ascertain whether this was also true of T cells by crossing VavP-*MYC*10 and VavP-*BCL2* mice (strain 69[24,27]). VavP-*BCL2* mice accumulate excessive numbers of both B- and T- lymphoid cells, including IgH class-switched B cells, and develop germinal center hyperplasia; a large number (37% to 50%, depending on the line) succumb to follicular lymphoma by 18 months of age.[24,27] Significantly, bitransgenic VavP-*MYC*10-*BCL2* mice had a much shorter lifespan (median, 13 weeks; n = 28) than mice expressing either transgene alone. Furthermore, BCL2 dramatically increased the rate of T-cell lymphomagenesis: of the sick mice autopsied, 47% (8 of 17) developed T-cell lymphomas and both of those tested were transplantable. The phenotype of these T-cell tumors varied: in 4 tumors, most cells were $CD4^+$ $CD8^+$, 1 tumor was $CD4^+$ $CD8^-$, 2 tumors had a mixture of these cell types, and another was $CD4^-$ $CD8^-$. Tumor-cell morphology varied in appearance from classic lymphoblastic to a more immunoblastic type (not shown), as observed for *MYC*17 T-cell lymphomas.[25] In all cases, the sick mice were highly leukemic and large tumor deposits were routinely seen throughout the hematopoietic system and in the liver, lung, and kidney.

Table 3. Macrophage colonies are increased in response to M-CSF in clonal cultures of VavP-*MYC* bone marrow cells

Stimulus	Mean no. colonies, ± SD					
	Blast	Granulocyte	Granulocyte-macrophage	Macrophage	Eosinophil	Megakaryocyte
Wild-type, 2 wk; n = 3						
GM-CSF	0	15 ± 4	7 ± 4	17 ± 4	2 ± 1	0
M-CSF	0	0.7 ± 0.6	3 ± 1	50 ± 17*	0	0
IL-3	8 ± 2	12 ± 4	8 ± 3	11 ± 12	2 ± 2	5 ± 2
SCF + IL-3 + EPO	8 ± 3	18 ± 6	12 ± 11	11 ± 12	2 ± 2	24 ± 5
***MYC*17, 2 wk; n = 3**						
GM-CSF	0	10 ± 2	4 ± 0	19 ± 8	2 ± 1	0
M-CSF	0	0	2 ± 2	158 ± 48*	0	0
IL-3	5 ± 2	9 ± 3	3 ± 3	13 ± 6	3 ± 3	6 ± 2
SCF + IL-3 + EPO	8 ± 3	7 ± 3	3 ± 2	13 ± 15	0.7 ± 1.2	11 ± 4
Wild-type, 8 wk; n = 4						
GM-CSF	0	16 ± 5	5 ± 2	31 ± 3	4 ± 2	0
M-CSF	0	3 ± 1	6 ± 4	49 ± 8*	0	0
IL-3	7 ± 4	19 ± 6	11 ± 3	15 ± 3	2 ± 1	7 ± 4
SCF + IL-3 + EPO	11 ± 6	21 ± 2	13 ± 3	17 ± 3	2 ± 1	28 ± 4
***MYC*10, 8 wk; n = 4**						
GM-CSF	0	19 ± 6	5 ± 2	29 ± 15	3 ± 3	0
M-CSF	0	3 ± 1	2 ± 1	109 ± 32*	0	0
IL-3	6 ± 1	16 ± 5	10 ± 3	22 ± 11	2 ± 1	6 ± 3
SCF + IL-3 + EPO	9 ± 4	20 ± 8	11 ± 6	15 ± 9	1 ± 2	23 ± 8

Bone marrow cells from healthy young mice of the age and genotype indicated were cultured in agar and stimulated with cytokines (GM-CSF, G-CSF, M-CSF, IL-3, EPO, SCF, G-CSF + SCF, TPO, Flt3L + LIF, SCF + IL-3 + EPO, IFNγ, IL-6) for 7 days. The resultant colonies were stained, examined for composition, and counted. The results with 4 different stimuli are shown as examples.

*Significant difference from wild-type controls was that the frequency of M-CSF-dependent macrophage colonies was increased for both *MYC*17 and *MYC*10 mice.

Table 4. Increased thymocyte proliferation in healthy young VavP-*MYC* mice

	2 weeks old				6 weeks old					
	Wild-type; n = 4		*MYC*17; n = 2		Wild-type; n = 5		*MYC*10; n = 5		*MYC*10^{hom}; n = 5	
	S phase	G_2/M phase	S phase	G_2/M phase	S phase	G_2/M phase	S phase	G_2/M phase	S phase	G_2/M phase
$CD4^+$ $CD8^{+}$*	11.6 ± 0.7	0.8 ± 0.1	15.9 ± 0.6	1.4 ± 0.2	7.6 ± 1	1.6 ± 0.3	9.2 ± 0.3	1.7 ± 0.3	10.3 ± 0.6	1.9 ± 0.4
P	—	—	.01	.01	—	—	.01	> .05	.001	> .05
$CD4^+$ $CD8^{-}$*	9.7 ± 0.4	0.8 ± 0.1	28.8 ± 0.8	1.3 ± 0.4	3.1 ± 0.9	1.1 ± 0.2	7.1 ± 0.2	1.3 ± 0.2	15.0 ± 0.5	1.5 ± 0.2
P	—	—	< .001	> .05	—	—	.001	> .05	< .001	> .05
$CD4^-$ $CD8^{+}$*	40.1 ± 1.6	0.9 ± 0.3	37.6 ± 0.5	0.8 ± 0.1	14.7 ± 2.4	1.3 ± 0.3	21.9 ± 1.2	1.5 ± 0.3	26.7 ± 1.1	1.6 ± 0.4
P	—	—	> .05	> .05	—	—	.01	> .05	< .001	> .05

P indicates *P* value calculated by *t* test; —, not applicable.
*Values in these rows are expressed as % ± SEM.

In the remaining sick *MYC*10-*BCL2* mice (9 of 17), no T-cell tumors were detected by flow cytometry or histologic analysis. Instead, their lymphoid organs were enlarged by a very large excess of small IgH class-switched B cells (mostly $CD19^+$ IgM^- IgD^+ κ light-chain$^+$). These cells did not appear to be neoplastic and the 3 cases tested were not transplantable. These class-switched B cells presumably reflect an exaggeration of the germinal center hyperplasia seen in VavP-*BCL2* mice.[27] An expansion of this population may be a constant feature of *MYC*10-*BCL2* mice, since it was also noted in some mice that developed T-cell tumors.

Discussion

Our comparison of 4 lines of transgenic mice expressing different levels of MYC in a range of hematopoietic cell types has revealed notable preneoplastic changes and marked effects of MYC levels on tumor phenotype.

Preneoplastic changes

The line with the highest expression, *MYC*17, had a dramatic preneoplastic phenotype, including a 3-fold enlarged spleen (with excess B-lymphoid and myeloid cells), a transient 10-fold increase in circulating leukocytes (both B-lymphoid and myeloid), and a substantial increase in bone marrow monocytes.[25] In contrast, the lower expression levels in *MYC*10 mice and *MYC*10^{hom} mice only modestly perturbed hematopoietic homeostasis (Table 1; not shown).

Megakaryocyte and platelet abnormalities were a notable feature of healthy young VavP-*MYC* mice, although the frequency and proliferative capacity of megakaryocyte progenitors in response to cytokines including SCF, IL-3, EPO, and TPO was normal (Table 3). Megakaryocytes were more abundant and larger (Figure 5A; Table 2) and their nuclei were abnormally large and complex, which suggests that MYC had promoted extra rounds of endoreplication, resulting in even greater polyploidy than is normal for this cell type.[31] Myc-driven endoreplication has previously been reported for mammalian keratinocytes[32] and some *Drosophila* cell types.[33] Since platelets in *MYC*17 and *MYC*10^{hom} mice were larger and less numerous than in normal littermates, MYC may also have retarded megakaryocyte maturation. Inhibition of differentiation by deregulated Myc has also been observed in other cell lineages.[4,16] Another prominent feature of bone marrow megakaryocytes was that the cytoplasm frequently contained multiple granulocytes, presumably due to increased emperipolesis. In this poorly understood process, megakaryocytes internalize other cells within demarcation membranes, a network that is continuous with extracellular fluid (see Bobik and Dabrowski,[34] McGarry et al,[35] and references therein). The "engulfed" cells therefore remain intact and able to exit. As in platelet α-granule disorders and myelofibrosis,[35-37] the reduced platelet production in VavP-*MYC* mice may result in the abnormal accumulation of granulocyte-attracting platelet proteins within megakaryocytes and augmented emperipolesis.

The bone marrow of young healthy VavP-*MYC* mice contained normal numbers of immature progenitor cells, as judged by the frequency of blast colonies that developed in semisolid agar cultures (Table 3). Committed megakaryocyte and myeloid progenitors were also normal in frequency and proliferative capacity, except for M-CSF–responsive macrophage progenitors, which were highly abnormal, generating large compact "cannonball" colonies (Figure 5B; Table 3). Comparable colonies were not seen with the other 2 cytokines able to stimulate macrophage colony formation (GM-CSF and IL-3; Table 3), suggesting that MYC may have led to the expansion of a specific subset of macrophage progenitors. The abnormal macrophage progenitors were not present in spleen, but were already present at birth in the neonatal liver of at least the *MYC17* mice (not shown). Recloning experiments (Figure 5C) indicated that they were not capable of full self-generation, although they did have greatly extended capacity for generating macrophage progenitors in response to M-CSF (but not GM-CSF). This feature was particularly marked in the case of the high MYC-expressing (*MYC*17) cells, which may account for the large excess of monocyte/macrophages found in the bone marrow of healthy young *MYC*17 mice.[25]

Tumor phenotype varies with MYC level

*MYC*17 mice all succumb to T-cell tumors,[25] most being mature $CD4^+$ $CD8^-$ lymphomas, which are rare in mouse models. The very rapid development of these tumors (Figure 2) masks the tumorigenic potential conferred by MYC on other hematopoietic cell types in these mice, since several other tumor classes, including pro–B-cell, progenitor-cell, and macrophage tumors are obtained in the absence of mature lymphocytes in the *Rag1*-null background.[25]

In the lines with much lower levels of VavP-*MYC* transgene expression (*MYC*10 and *MYC*12), morbidity is primarily due to slow-developing disseminated histiocytic monocyte/macrophage tumors (Figures 2, 3A-B). This suggests that the macrophage lineage is particularly susceptible to MYC-induced transformation. It is tempting to speculate that these tumors arise from the abnormal macrophage progenitors seen in preneoplastic mice. The VavP-*MYC* macrophage tumors resemble human histiocytic sarcoma (which, like the VavP-*MYC* tumors, can present in the skin) and its disseminated form, malignant histiocytosis.[38] Since tumors develop in *MYC*10 and *MYC*12 mice within an experimentally acceptable latent period and the penetrance is high, these lines may be valuable models for these rare but generally incurable human

neoplasms. MYC involvement in these in these neoplasms has not been described, and our data indicate that such an analysis may be worthwhile.

The 2-fold increase in MYC obtained by generating mice homozygous for the *MYC*10 locus led to a remarkable difference in pathogenic outcome. The median survival was 13 weeks rather than 41 weeks (Figure 2) and the *MYC*10^{hom} mice succumbed to lymphoblastic T-cell lymphomas (Figure 3C-D) rather than histiocytic monocyte/macrophage tumors. Curiously, although the preneoplastic impact of MYC on T cells (proliferation, growth, and apoptosis) in *MYC*10^{hom} mice was greatest in the CD4$^-$ CD8$^+$ and, in particular, the CD4$^+$ CD8$^-$ thymocyte population (Figure 4; Table 4), the tumors were almost all CD4$^+$ CD8$^+$ pre–T-cell lymphomas, as is typical in other MYC transgenic lines that are prone to T-cell tumors.[21,39] In contrast, most high-expressing *MYC*17 mice succumb to mature CD4$^+$ CD8$^-$ tumors,[25] suggesting that malignant transformation of this cell type requires higher levels of MYC.

Strikingly, crossing a *BCL2* transgene into *MYC*10 mice greatly enhanced their susceptibility to T-cell lymphomas (50% versus 7%). This suggests that the malignant transformation of MYC-driven T cells depends, at least in part, on accumulating antiapoptotic mutation(s) and that, in conjunction with an antiapoptotic mutation, even the modest proliferative and cell-growth effects of low-level MYC expression (Figure 4; Table 4) can drive efficient T-cell lymphomagenesis. The differing levels of MYC in VavP-*MYC* mice all induce apoptosis in cultured T cells (Figure 4C), and the mechanism is likely to be similar. However, the observations that *MYC*10 mice only efficiently developed T-cell tumors when an antiapoptotic mutation was enforced and that all *MYC*10^{hom} and *MYC*17 mice rapidly developed T-cell lymphomas suggest that the odds of spontaneously developing cooperating antiapoptotic mutations are proportional to the level of MYC.

The mechanism of Myc-induced apoptosis is still poorly understood,[6] but involves resetting the life/death rheostat regulated by the Bcl2 family.[20,40] Myc up-regulates the tumor suppressor p19Arf, which in turn leads to increased p53[41] and transcriptional activation of 2 proapoptotic Bcl2 relatives, the BH3-only proteins Puma and Noxa.[42,43] Myc also elevates the p53-independent expression of another BH3-only protein, Bim,[20] and, in parallel, the levels of antiapoptotic Bcl2 and Bclx$_L$ proteins diminish.[20,44] Thus, Myc increases the ratio of proapoptotic to antiapoptotic proteins, lowering the threshold for induction of apoptosis. To progress to malignancy, cells with constitutive MYC expression must overcome their predilection to apoptosis, and this can be achieved experimentally in Eμ-Myc mice either by imposing expression of Bcl2[18] or Bclx$_L$,[45] or by loss of p53,[46] p19Arf,[19,46] Bim,[20] or Puma.[47] Pertinently, a high proportion of spontaneous Eμ-Myc lymphomas[19] and Burkitt lymphomas[48] exhibit mutations inactivating the p19Arf/Mdm2/p53 axis. Furthermore, 2 MYC point mutants isolated from Burkitt lymphomas are defective at inducing Bim (while still retaining ability to stimulate proliferation and p53 activation),[49] and loss of *BIM* is a common feature of human mantle-cell lymphoma.[50]

Implications

Our studies have demonstrated a remarkable difference in pathogenic phenotype that is dependent on the level of MYC expression. More specifically, the results suggest that macrophages are susceptible to malignant transformation at even low levels of MYC, and that there is a sharp threshold level of MYC that must be surpassed for efficient T-cell lymphomagenesis.

Once this threshold is surpassed, as in *MYC*10^{hom} mice, the acquisition of T-cell–relevant synergistic mutations appears to be greatly facilitated. This may simply be the consequence of the increased number of cell divisions. Alternatively, higher levels of MYC expression could have more direct effects, such as altered expression of pathologic target genes due to occupation of low affinity and aberrant promoter binding sites.[1,2] Higher levels of MYC may also promote genomic instability.[5] Fine-tuning the level of deregulated MYC expression may be an important mechanism in the progression of human cancers. For example, mutations in MYC that are selected during the progression of Burkitt lymphoma not only abrogate the induction of Bim[49] but also increase the stability of MYC.[11-13]

Since the tumor phenotype of *MYC*10 mice is so sensitive to MYC levels, this line should be a uniquely responsive indicator strain to examine the lymphomagenic impact of mutations in genes that may influence MYC stability (for example, *GSK3B*, *PIN1*, *PP2A*, *FBW7*, *and SKP2*, which regulate MYC phosphorylation and subsequent degradation[11,12]) or activity (for example, the *MAD* family of antagonists[51]). Furthermore, in *MYC*10^{hom} mice, agents that decrease the level of MYC even 2-fold should dramatically reduce the incidence of T-cell lymphomas. Hence, these mice may prove to be a valuable strain in which to test therapeutics targeted at pathways regulating MYC stability or activity.[22]

In summary, these VavP-*MYC* transgenic mice represent valuable new tools to study the mechanisms of leukemogenesis, to search for and test putative cooperating mutations, and to investigate the impact of chemotherapeutics on tumors of the T lymphoid and monocyte/macrophage lineages. They also provide the means to compare MYC targets at different expression levels and in multiple hematopoietic cell types.

Acknowledgments

We thank J. Adams for helpful discussions, A. Strasser for his gift of antibodies, and A. Wiegmans for technical assistance.

References

1. Fernandez PC, Frank SR, Wang L, et al. Genomic targets of the human c-Myc protein. Genes Dev. 2003;17:1115-1129.
2. Li Z, Van Calcar S, Qu C, Cavenee WK, Zhang MQ, Ren B. A global transcriptional regulatory role for c-Myc in Burkitt's lymphoma cells. Proc Natl Acad Sci U S A. 2003;100:8164-8169.
3. Grandori C, Cowley SM, James LP, Eisenman RN. The Myc/Max/Mad network and the transcriptional control of cell behavior. Ann Rev Cell Dev Biol. 2000;16:653-699.
4. Henriksson M, Luscher B. Proteins of the Myc network: essential regulators of cell growth and differentiation. Adv Cancer Res. 1996;68:109-182.
5. Soucek L, Evan G. Myc-Is this the oncogene from Hell? Cancer Cell. 2002;1:406-408.
6. Nilsson JA, Cleveland JL. Myc pathways provoking cell suicide and cancer. Oncogene. 2003;22:9007-9021.
7. Cory S. Activation of cellular oncogenes in hemopoietic cells by chromosome translocation. Adv in Cancer Res. 1986;47:189-234.
8. Marcu KB, Bossone SA, Patel AJ. myc function and regulation. Annu Rev Biochem. 1992;61:809-860.
9. Sanchez-Beato M, Sanchez-Aguilera A, Piris MA. Cell cycle deregulation in B-cell lymphomas. Blood. 2003;101:1220-1235.
10. Boxer LM, Dang CV. Translocations involving c-*myc* and c-*myc* function. Oncogene. 2001;20:5595-5610.
11. Amati B. Myc degradation: dancing with ubiquitin ligases. Proc Natl Acad Sci U S A. 2004;101:8843-8844.
12. Dominguez-Sola D, Dalla-Favera R. PINning

down the c-Myc oncoprotein. Nat Cell Biol. 2004; 6:288-289.

13. Sears RC. The life cycle of c-Myc: from synthesis to degradation. Cell Cycle. 2004;3:1133-1137.
14. Adams JM, Harris AW, Pinkert CA, et al. The c-*myc* oncogene driven by immunoglobulin enhancers induces lymphoid malignancy in transgenic mice. Nature. 1985;318:533-538.
15. Harris AW, Pinkert CA, Crawford M, Langdon WY, Brinster RL, Adams JM. The Eμ-*myc* transgenic mouse: a model for high-incidence spontaneous lymphoma and leukemia of early B cells. J Exp Med. 1988;167:353-371.
16. Langdon WY, Harris AW, Cory S, Adams JM. The c-*myc* oncogene perturbs B lymphocyte development in Eμ-*myc* transgenic mice. Cell. 1986;47: 11-18.
17. Adams JM, Harris AW, Strasser A, Ogilvy S, Cory S. Transgenic models of lymphoid neoplasia and development of a pan-hematopoietic vector. Oncogene. 1999;18:5268-5277.
18. Strasser A, Harris AW, Bath ML, Cory S. Novel primitive lymphoid tumours induced in transgenic mice by cooperation between *myc* and *bcl*-2. Nature. 1990;348:331-333.
19. Eischen CM, Weber JD, Roussel MF, Sherr CJ, Cleveland JL. Disruption of the ARF-Mdm2-p53 tumor suppressor pathway in Myc-induced lymphomagenesis. Genes Dev. 1999;13:2658-2669.
20. Egle A, Harris AW, Bouillet P, Cory S. Bim is a suppressor of Myc-induced mouse B cell leukemia. Proc Natl Acad Sci U S A. 2004;101:6164-6169.
21. Felsher DW, Bishop JM. Reversible tumorigenesis by MYC in hematopoietic lineages. Mol Cell. 1999;4:199-207.
22. Bachireddy P, Bendapudi PK, Felsher DW. Getting at MYC through RAS. Clin Cancer Res. 2005;11:4278-4781.
23. Ogilvy S, Metcalf D, Gibson L, Bath ML, Harris AW, Adams JM. Promoter elements of *vav* drive transgene expression in vivo throughout the hematopoietic compartment. Blood. 1999;94:1855-1863.
24. Ogilvy S, Metcalf D, Print CG, Bath ML, Harris AW, Adams JM. Constitutive bcl-2 expression throughout the hematopoietic compartment affects multiple lineages and enhances progenitor cell survival. Proc Natl Acad Sci U S A. 1999;96: 14943-14948.
25. Smith DP, Bath ML, Harris AW, Cory S. T-cell lymphomas mask slower developing B-lymphoid and myeloid tumors in transgenic mice with broad hematopoietic expression of MYC. Oncogene. 2005;24:3544-3553.
26. Bath ML. Simple and efficient in vitro fertilization with cryopreserved C57BL/6J mouse sperm. Biol Reprod. 2003;68:19-23.
27. Egle A, Harris AW, Bath ML, O'Reilly L, Cory S. VavP-*Bcl2* transgenic mice develop follicular lymphoma preceded by germinal center hyperplasia. Blood. 2004;103:2276-2283.
28. Metcalf D, Di Rago L, Mifsud S. Synergistic and inhibitory interactions in the in vitro control of murine megakaryocyte colony formation. Stem Cells. 2002;20:552-560.
29. Alexander WS, Schrader JW, Adams JM. Expression of the c-*myc* oncogene under control of an immunoglobulin enhancer in Eμ-*myc* transgenic mice. Mol Cell Biol. 1987;7:1436-1444.
30. Kogan SC, Ward JM, Anver MR, et al. Bethesda proposals for classification of nonlymphoid hematopoietic neoplasms in mice. Blood. 2002;100: 238-245.
31. Shivdasani RA. Molecular and transcriptional regulation of megakaryocyte differentiation. Stem Cells. 2001;19:397-407.
32. Gandarillas A, Davies D, Blanchard JM. Normal and c-Myc-promoted human keratinocyte differentiation both occur via a novel cell cycle involving cellular growth and endoreplication. Oncogene. 2000;19:3278-3789.
33. Edgar BA, Orr-Weaver TL. Endoreplication cell cycles: more for less. Cell. 2001;105:297-306.
34. Bobik R, Dabrowski Z. Emperipolesis of marrow cells within megakaryocytes in the bone marrow of sublethally irradiated mice. Ann Hematol. 1995; 70:91-95.
35. McGarry MP, Reddington M, Jackson CW, Zhen L, Novak EK, Swank RT. Increased incidence and analysis of emperipolesis in megakaryocytes of the mouse mutant gunmetal. Exp Mol Pathol. 1999;66:191-200.
36. Schmitt A, Jouault H, Guichard J, Wendling F, Drouin A, Cramer EM. Pathologic interaction between megakaryocytes and polymorphonuclear leukocytes in myelofibrosis. Blood. 2000;96: 1342-1347.
37. White JG. Structural defects in inherited and giant platelet disorders. Adv Hum Genet. 1990;19:133-234.
38. Pileri SA, Grogan TM, Harris NL, et al. Tumours of histiocytes and accessory dendritic cells: an immunohistochemical approach to classification from the International Lymphoma Study Group based on 61 cases. Histopathology. 2002;41:1-29.
39. Stewart M, Cameron E, Campbell M, et al. Conditional expression and oncogenicity of c-*myc* linked to a CD2 gene dominant control region. Int J Cancer. 1993;53:1023-1030.
40. Cory S, Huang DCS, Adams JM. The Bcl-2 family: roles in cell survival and oncogenesis. Oncogene. 2003;22:8590-8607.
41. Sherr CJ, McCormick F. The RB and p53 pathways in cancer. Cancer Cell. 2002;2:103-112.
42. Oda E, Ohki R, Murasawa H, et al. Noxa, a BH3-only member of the bcl-2 family and candidate mediator of p53-induced apoptosis. Science. 2000;288:1053-1058.
43. Nakano K, Vousden KH. *PUMA*, a novel proapoptotic gene, is induced by p53. Mol Cell. 2001;7: 683-694.
44. Eischen CM, Woo D, Roussel MF, Cleveland JL. Apoptosis triggered by *myc*-induced suppression of Bcl-X_L or Bcl-2 is bypassed during lymphomagenesis. Mol Cell Biol. 2001;21:5063-5070.
45. Swanson PJ, Kuslak SL, Fang W, et al. Fatal acute lymphoblastic leukemia in mice transgenic for B cell-restricted bcl-x_L and c-*myc*. J Immunol. 2004;172:6684-6691.
46. Schmitt CA, McCurrach ME, de Stanchina E, Wallace-Brodeur RR, Lowe SW. *INK4a/ARF* mutations accelerate lymphomagenesis and promote chemoresistance by disabling p53. Genes Dev. 1999;13:2670-2677.
47. Hemann MT, Zilfou JT, Zhao Z, Burgess DJ, Hannon GJ, Lowe SW. Suppression of tumorigenesis by the p53 target PUMA. Proc Natl Acad Sci U S A. 2004;101:9333-9338.
48. Blum KA, Lozanski G, Byrd JC. Adult Burkitt leukemia and lymphoma. Blood. 2004;104:3009-3020.
49. Hemann MT, Bric A, Teruya-Feldstein J, et al. Evasion of the p53 tumour surveillance network by tumour-derived MYC mutants. Nature. 2005; 436:807-811.
50. Tagawa H, Karnan S, Suzuki R, et al. Genome-wide array-based CGH for mantle cell lymphoma: identification of homozygous deletions of the pro-apoptotic gene *BIM*. Oncogene. 2005;24:1348-1358.
51. Nilsson JA, Cleveland JL. MNT: master regulator of the Max network. Cell Cycle. 2004;3:588-590.